DTU Library

Recovery in heavily deformed nickel during room temperature storage

Zhang, Yubin; Mishin, Oleg; Kamikawa, Naoya; Godfrey, A.

Published in:
Proceedings of the Risø International Symposium on Materials Science

Publication date:
2014

RECOVERY IN HEAVILY DEFORMED NICKEL DURING ROOM TEMPERATURE STORAGE

Y.B. Zhang*, O.V. Mishin*, N. Kamikawa**, A. Godfrey***

* Danish-Chinese Center for Nanometals, Department of Wind Energy, Technical University of Denmark, Risø Campus, Roskilde 4000, Denmark
** Institute for Materials Research, Tohoku University, 2-1-1 Katahira, Aoba-ku, Sendai 980-8577, Japan
*** Key Laboratory of Advanced Materials (MOE), School of Materials Science and Engineering, Tsinghua University, Beijing 100084, PR China

ABSTRACT

The microstructural evolution in pure nickel cold deformed to a von Miss strain of 4.8 using an accumulative roll bonding process has been monitored by investigating selected regions after different periods of room-temperature storage. It is found that the quality of electron backscatter diffraction (EBSD) patterns improves during the storage, with no appreciable migration of grain boundaries and triple junctions, as revealed by EBSD and transmission electron microscopy. Tensile test data demonstrate that the strength decreases during the storage. It is suggested that these changes reflect an overall reduction of the dislocation density. The relationship between the microstructure of the as-deformed and recovered sample and their mechanical properties is discussed.

1. INTRODUCTION

Nanostructured materials produced by severe plastic deformation (SPD) processes, such as cold rolling and accumulative roll bonding (ARB), to very high strains are known to contain large frequencies of deformation-induced high angle boundaries (HABs) and high densities of interior dislocations (Azushima, Kopp, Korhonen, Yang, Micari, Lahoti and Yanagida 2008; Hughes and Hansen 2000; Tsuji, Ito, Saito and Minamino 2002). The energy stored in such materials in the form of boundaries and dislocations is rather high, which makes the thermal stability of nanostructured materials poor (Gao, Starink and Langdon 2009; Knudsen, Cao, Godfrey, Liu and Hansen 2008). For example, partial recrystallization was found to occur in nanostructured copper and silver processed by SPD even during room temperature (RT) storage (Mishin and Godfrey 2008; Gubicza, Chinh, Lábár, Hegedüs and Langdon 2010; Lin, Zhang, Tao, Pantleon and Juul Jensen 2014). Whereas heavily deformed commercially pure Al is not prone to recrystallization at RT, its microstructure is still not absolutely stable, as annihilation of dislocations both between deformation-induced lamellar boundaries and within the boundaries, and even triple junction motion may take place during long-term RT storage (Yu, Hansen and Huang 2011; Tianbo Yu, Hansen and Huang 2012). Furthermore, it has been suggested that a reduction in the dislocation density can be responsible for an interesting phenomenon of hardening by annealing observed for some Al and IF-steel samples processed by ARB (Huang, Hansen and Tsuji 2006; Kamikawa, Zhang, Huang and Hansen 2008; Kamikawa, Huang and Hansen 2010). These observations imply that processes occurring during low-temperature annealing and RT storage may significantly affect the mechanical behavior of heavily deformed materials.

The aim of the present work is to investigate if any considerable changes take place during long-term RT storage in the microstructure of heavily deformed nickel. The material chosen for this study is a pure nickel sample processed by ARB (Zhang, Mishin and Godfrey 2014). The microstructural characterization of this sample after different periods of RT storage is complemented by analysis of the evolution of its strength and hardness.

2. EXPERIMENTAL

A 2-mm thick strip of pure (99.967%) nickel with a fully recrystallized microstructure and a nearly random texture was used as the initial material (Zhang, Mishin, Kamikawa, Godfrey, Liu, and Liu 2013; Zhang et al. 2014). The average grain size measured by EBSD in this sample was ~20 μm (including annealing twins). The strip was cold-rolled 50% on well-lubricated rolls with a diameter of 310 mm. The sample obtained after this rolling pass was cut in half. After degreasing and wire-brushing, the halves were stacked and rolled 50% again, to create a bonding between the halves. After each roll-bonding cycle, the sample was quenched in water. This roll-bonding operation was conducted repeatedly to reach a total von Mises strain of $\varepsilon_{vM} = 4.8$. The sample was stored at RT after deformation.

Several regions in the deformed sample were first characterized using both transmission electron microscopy (TEM) and electron backscatter diffraction (EBSD) techniques approximately 4 months after the deformation. The same regions were characterized again after 4.5 years of RT storage. Tensile specimens with a gauge length of 10 mm, a width of 5 mm and a thickness of 1 mm were prepared after almost 4 months, 8 months and 4.5 years of storage. In addition, one specimen was prepared after annealing at 200°C for 1 h. Tensile tests were conducted by pulling the specimens along the rolling direction (RD) at a constant crosshead speed of 0.5 mm / minute, which corresponds to an initial strain rate of 8.3×10^{-4} s^{-1}.

3. RESULTS

A TEM image of the deformed microstructure in the center region of the sample after 4 months of storage is shown in Fig. 1a. The microstructure is dominated by lamellar structures formed by extended boundaries aligned almost parallel to the rolling plane. Evidence of localized shear at 25 – 40° to the RD is also observed in this sample. The lamellae are further subdivided by dislocation cell boundaries. The cell interior is characterized in Fig.1a by a high dislocation density. The average boundary spacing along the sample normal direction (ND), d_{ND}, for all boundaries is ~120 nm in this region.

The microstructure in the same region after storage for 4.5 years is shown in Fig.1b. By comparing the microstructure before and after this additional storage, no appreciable change is revealed in the position of the lamellar and interconnected boundaries. It can therefore be concluded that no substantial triple junction motion has occurred during the storage. Although no measurements of the dislocation density was conducted in the as-prepared TEM foil, it appears that cell interiors in this foil are characterized by a higher density of dislocations than those after 4.5 years (cf. Fig.1a and Fig.1b). Certain differences are also observed in the EBSD data collected after the different periods of storage (cf. Fig.2a,b and Fig.2c,d). Comparing the band contrast maps in Fig.2a and Fig.2c, it is apparent that the quality of EBSD patterns improves significantly during the long-term storage. Also, the EBSD indexing rate improves from 82% after 4 months to 89% after the long-term storage.

It can be noticed that the lamellar boundaries in Fig. 2a,b appear zigzagging along their length, whereas this phenomenon is less pronounced in Fig. 2c,d. Apparently, the zigzagging shape is an artifact due to the orthogonal grid implemented for our EBSD scans. The fact that this artifact biases the boundary images in the two maps differently can be explained by different scan orientations: the data set for Fig. 2a,b was collected by scanning along the ND, while the data set for Fig. 2c,d was produced by scanning along the RD.

The boundary spacing measured along the ND in the EBSD maps shown in Fig.2a,b and Fig.2c,d is 160 nm, i.e. somewhat larger than the value obtained in the TEM experiment. Larger boundary spacings by EBSD are typically obtained in similar comparative studies of deformed microstructures because TEM is capable of revealing dislocation boundaries even with very low misorientations which are ignored in the EBSD maps (Godfrey, Mishin and Liu 2006; Mishin, Östensson and Godfrey 2006). To verify that the unchanged boundary spacing during the long-term storage is not unique to the thin foil, new EBSD maps were collected in a bulk specimen after 6 years of storage. Again, it was found that the average boundary spacing was about 160 nm also in the bulk.

Fig. 1. TEM images showing the microstructure in one region of the ARB-processed nickel sample investigated after different periods of storage: (a) 4 months and (b) 4.5 years after deformation.

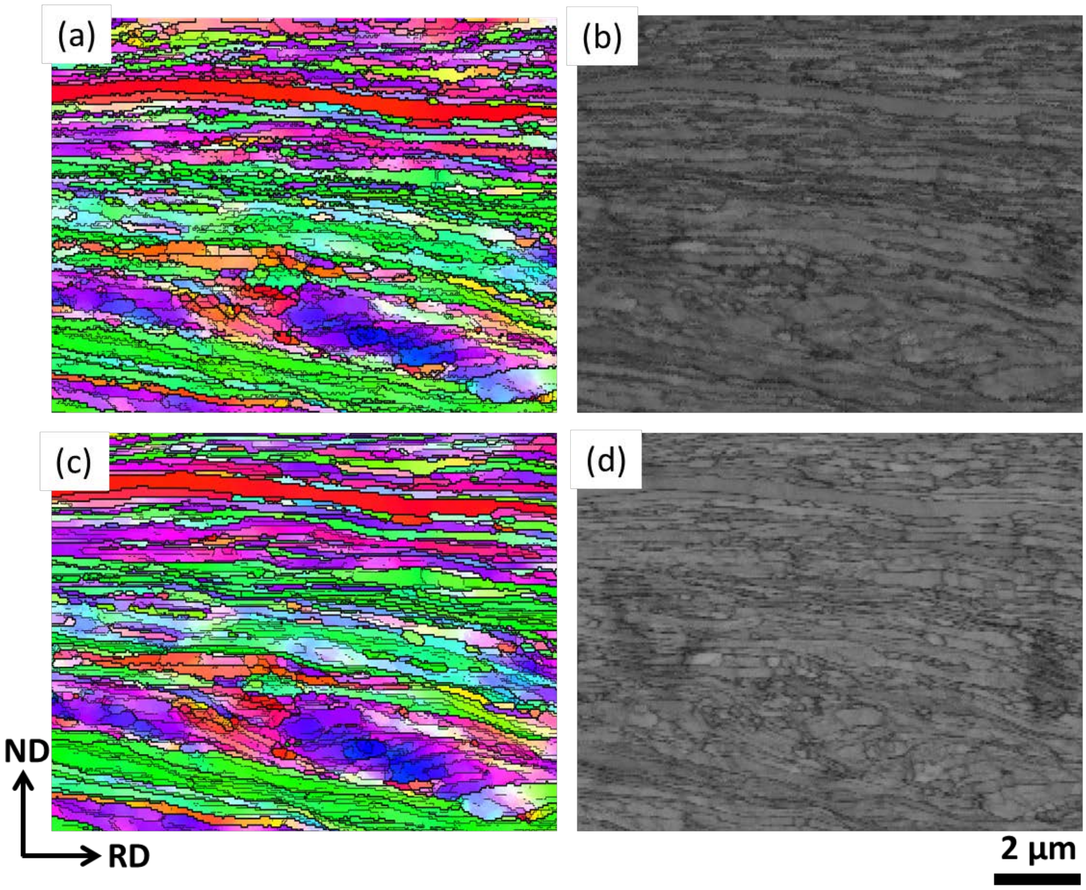

Fig. 2. EBSD maps from the ARB-processed nickel sample investigated after different periods of storage: (a) 4 months and (b) 4.5 years after deformation. Orientations in (a) and (c) are colored according to the inverse pole figure. Black lines correspond to misorientations >2°. (b) and (d) represent the band contrast in EBSD patterns.

Strain-stress curves for the sample tested after different periods of storage are shown in Fig. 3. It is seen that the strength gradually decreases during the entire storage period and that after 4.5 years of storage the 0.2% proof stress is reduced by ~100 MPa. The reduction in the ultimate tensile strength (UTS) is less significant.

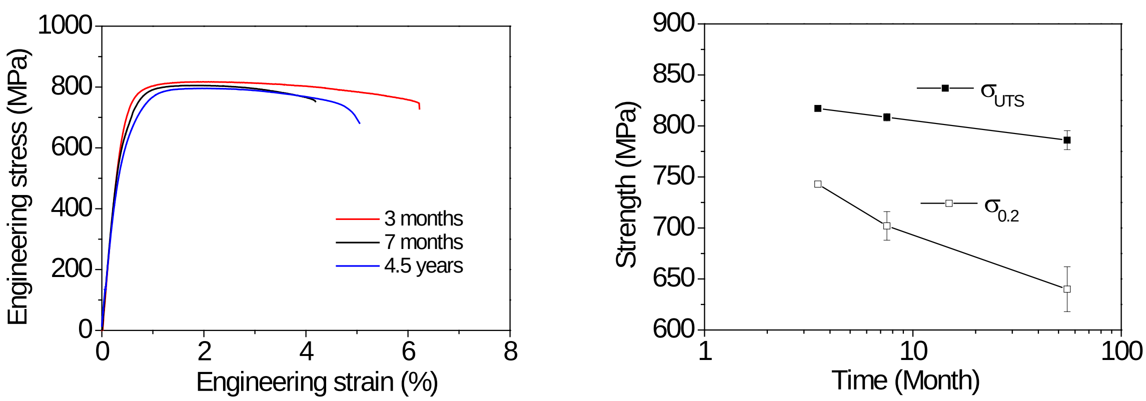

(a) (b)

Fig. 3. Tensile test data for the deformed ARB nickel sample after different storage periods: (a) stress-strain curves; (b) the 0.2% proof stress and ultimate tensile strength.

4. DISCUSSION

4.1. Recovery during RT storage. Compared to nanostructured Al, Cu and Ag produced by SPD, in which triple junction motion or even recrystallization were observed after long-term RT storage (Gubicza et al. 2010; Lin et al. 2014; Mishin and Godfrey 2008; Yu et al. 2011; Yu et al. 2012), the microstructure of our nanostructured nickel sample appears more stable, as no appreciable boundary migration or triple junction motion was revealed in this ARB-processed material even after 4.5 years of storage. Despite this, the strength decreases during the storage. This change in strength can be analyzed using the following equation (Hansen 2004; Kamikawa, Huang, Tsuji and Hansen 2009):

$$\sigma = \sigma_0 + M\alpha Gb\sqrt{\rho_0 + \frac{3(1-f)\theta_{av}}{bd_{av}}} + k_{HP}\sqrt{\frac{f}{d_{av}}} \tag{1}$$

where k_{HP} is the slope in the Hall-Petch plot for annealed polycrystalline nickel (159 MPa μm$^{0.5}$ according to Thompson 1975); f is the fraction of boundaries with misorientation angles above a critical angle θ_{c} (estimated to be ~ 4 – 6°, see Zhang et al. 2013); $M \approx 3$ is the Taylor factor; $\alpha \approx 0.24$ is a constant; G = 79 GPa is the shear modulus; b = 0.249 nm is the Burgers vector; θ_{av} is the average misorientation angle for boundaries with misorientations below θ_{c}; d_{av} is the average boundary spacing measured along random lines; σ_0 is the friction stress; and ρ_0 is the dislocation density within cells.

In our work, the reduction in the 0.2% proof stress during the storage is known, $\Delta\sigma \approx 100$ MPa. For cases when there is no migration of boundaries and triple junctions, Δf, $\Delta\theta_{\mathrm{av}}$, and Δd_{av} are 0. Based on Eq. (1), the change in dislocation density $\Delta\rho$ can then be expressed as:

$$\Delta\rho = \frac{(\sigma_1 - \sigma_0 - \sigma_{HP})^2 - (\sigma_2 - \sigma_0 - \sigma_{HP})^2}{(M\alpha Gb)^2} \tag{2}$$

where $\sigma_{HP} = k_{HP}\sqrt{f/d_{av}}$, σ_1 and σ_2 are the yield stress after 4 months and after 4.5 years of storage, respectively. According to Eq. (2), the reduction in σ by 100 MPa corresponds to a 5×10^{14} m^{-2} decrease in the overall dislocation density.

The density of interior dislocations in severely deformed nickel is typically of an order of 10^{14} m^{-2} (Zhang, Huang and Hansen 2008), i.e. smaller than the predicted loss in the overall dislocation density. Considering that the density of such dislocations is still significant after the long-term storage, it is apparent that the reduction in the density of these dislocations alone is not sufficient to account for the observed loss in strength. It is suggested that a reduction in the density of so-called redundant dislocations within deformation-induced boundaries containing a high density of dipoles and multipoles (Hughes, Hansen and Bammann 2003; Krasilnikov, Lojkowski, Pakiela and Valiev 2005; Knudsen et al. 2008) should also be taken into account. According to Krasilnikov et al. 2005, the density of redundant dislocations in heavily deformed nickel is ~10^{14} m^{-2}, i.e. similar to that of the interior dislocations. It is, therefore, reasonable to suggest that the reduction in strength revealed during the long-term RT storage is due a combined loss of both interior dislocations and redundant dislocations within deformation-induced boundaries.

4.2. Strengthening mechanisms in nanostructured nickel. In general, long-term RT storage can be considered as an annealing process, termed “self-annealing” in some studies (Gubicza et al. 2010). The decrease in strength during self-annealing implies that nanostructured nickel behaves similar to conventional materials, i.e. that hardening by annealing reported for some heavily deformed Al samples and IF steel (Huang et al. 2006; Kamikawa et al. 2008; Kamikawa et al. 2010) does not occur in heavily deformed nickel. Possible reasons for this can be that (i) the density of interior dislocations in the nickel sample was initially higher than that in Al; and (ii) the RT annealing treatment did not remove enough dislocations to result in a lack of dislocation sources during tensile deformation necessary for hardening by annealing to occur. It should also be mentioned that in contrast to the studies of Huang et al. 2006, Kamikawa et al. 2008 and Kamikawa et al. 2010, where an increase in strength was seen in annealed samples with a coarsened microstructure, no coarsening during self-annealing was observed in the present work.

To understand whether the absence of the hardening-by-annealing effect is not restricted to RT self-annealing, a sample annealed at 200°C for 1 h after ARB was also investigated in this work. The microstructure of this annealed sample was slightly coarser than that after deformation, and no hardening was observed. On the contrary, the annealed sample was ~5% softer and the 0.2% proof stress after the annealing treatment was ~150 MPa lower than that for the deformed condition. Similar softening behavior has been observed in nanostructured nickel obtained by heavy deformation (Krasilnikov et al. 2005; Lee, Chang and Kao 2005). It can therefore be concluded that in contrast to the Al and IF-steel samples studied by Huang et al. 2006, Kamikawa et al. 2008 and Kamikawa et al. 2010, where a dislocation source-limitation mechanism was proposed to increase the strength by annealing, no evidence of this mechanism is found in heavily deformed nanostructured nickel under the conditions used in this study, in which the strength is only governed by the standard dislocation and boundary strengthening mechanisms. This may be related to the higher dislocation density in deformed Ni such that the window for observing a source hardening effect may be considerably narrower in Ni than in Al and IF-steel.

5. CONCLUSIONS

The long-term microstructural stability has been investigated in a nanostructured nickel sample produced by the ARB technique. It has been found that the deformed microstructure is comparatively stable, where no appreciable boundary migration and triple junction motion are observed even after 4.5 years of room temperature storage. The decrease in strength observed during the storage is attributed to a reduction in the overall dislocation density. It is estimated that after 4.5 years the dislocation density decreases by about 5×10^{14} m^{-2} as compared to that in the material investigated only 4 months after deformation. This reduction is consistent with the improved quality of EBSD patterns and higher indexing rate. It is found that annealing at 200°C for 1 h also results in reduced strength, which is similar to previous results obtained on nickel, heavily deformed and subsequently annealed at similar temperatures. Thus, hardening by annealing, reported for some heavily deformed Al and IF-steel samples, is not revealed for nickel under the conditions used in this study.

ACKNOWLEDGEMENTS

The authors gratefully acknowledge the support from the Danish National Research Foundation (Grant No DNRF86-5) and the National Natural Science Foundation of China (Grant No. 51261130091) to the Danish-Chinese Center for Nanometals, within which this work has been performed. NK also thanks the financial support from the Grant-in-Aid for Scientific Research on Innovative Area “Bulk Nanostructured Metals” (No. 22102006) through the Ministry of Education, Culture, Sports, Science and Technology of Japan.

REFERENCES

Azushima, A., Kopp, R., Korhonen, A., Yang, D.Y., Micari, F., Lahoti, G.D. and Yanagida, A. (2008). Severe plastic deformation (SPD) processes for metals. CIRP Annals – Manufact. Technol., 57, 716–735.

Gao, N., Starink, M.J. and Langdon, T.G. (2009). Using differential scanning calorimetry as an analytical tool for ultrafine grained metals processed by severe plastic deformation. Mater. Sci. Technol., 25, 687–698.

Godfrey, A., Mishin, O.V. and Liu, Q. (2006). Processing and interpretation of EBSD data gathered from plastically deformed metals. Mater. Sci. Technol. 22, 1263–1270.

Gubicza, J., Chinh, N.Q., Lábár, J.L., Hegedűs, Z. and Langdon, T.G. (2010). Principles of self-annealing in silver processed by equal-channel angular pressing: The significance of a very low stacking fault energy. Mater. Sci. Eng. A, 527, 752–760.

Hansen, N. (2004). Hall–Petch relation and boundary strengthening. Scr. Mater., 51, 801–806.

Huang, X., Hansen, N. and Tsuji, N. (2006). Hardening by annealing and softening by deformation in nanostructured metals. Science (New York, N.Y.), 312(5771), 249–51.

Hughes, D.A., Hansen, N. and Bammann, D. (2003). Geometrically necessary boundaries, incidental dislocation boundaries and geometrically necessary dislocations. Scr. Mater., 48, 147–153.

Hughes, D.A. and Hansen, N. (2000). Microstructure and strength of nickel. Acta Mater., 48, 2985–3004.

Kamikawa, N., Huang, X., Tsuji, N. and Hansen, N. (2009). Strengthening mechanisms in nanostructured high-purity aluminium deformed to high strain and annealed. Acta Materialia, 57(14), 4198–4208.

Kamikawa, N., Huang, X. and Hansen, N. (2010). Dislocation-source hardening in nano-structured steel produced by severe plastic deformation. Mater. Sci. Forum, 638-642, 1959–1964.

Kamikawa, N., Zhang, H., Huang, X. and Hansen, N. (2008). Microstructure and mechanical properties of nanostructured metals produced by high strain deformation, Mater. Sci. Forum, 579, 135–145.

Knudsen, T., Cao, W.Q., Godfrey, A., Liu, Q. and Hansen, N. (2008). Stored energy in nickel cold rolled to large strains, measured by calorimetry and evaluated from the microstructure. Metall. Mater. Trans. A, 39, 430–440.

Krasilnikov, N., Lojkowski, W., Pakiela, Z. and Valiev, R.Z. (2005). Tensile strength and ductility of ultra-fine-grained nickel processed by severe plastic deformation. Mater. Sci. Eng. A, 397, 330–337.

Lee, T.R., Chang, C.P. and Kao, P.W. (2005). The tensile behavior and deformation micro-structure of cryo-rolled and annealed pure nickel. Mater. Sci. Eng. A, 408, 131–135.

Lin, F.X., Zhang, Y.B., Tao, N., Pantleon, W. and Juul Jensen, D. (2014). Effects of heterogeneity on recrystallization kinetics of nanocrystalline copper prepared by dynamic plastic deformation. Acta Mater., 72, 252–261.

Mishin, O.V. and Godfrey, A. (2008). Microstructure of ECAE-processed copper after long-term room-temperature storage. Metall. Mater. Trans. A, 39, 2923–2930.

Mishin, O.V., Östensson, L. and Godfrey, A. (2006). Comparative microstructural characterization of a friction-stir-welded aluminum alloy using TEM and SEM-based techniques. Metall. Mater. Trans. A, 37, 489–496.

Thompson, A. (1975). Yielding in nickel as a function of grain or cell size. Acta Metall., 23, 1337-1342.

Tsuji, N., Ito, Y., Saito, Y. and Minamino, Y. (2002). Strength and ductility of ultrafine grained aluminum and iron produced by ARB and annealing. Scr. Mater., 47, 893–899.

Yu, T., Hansen, N. and Huang, X. (2011). Recovery by triple junction motion in aluminium deformed to ultrahigh strains. Proc. Royal Soc. A, 467, 3039–3065.

Yu, T., Hansen, N. and Huang, X. (2012). Recovery mechanisms in nanostructured aluminium. Phil. Mag., 92, 4056–4074.

Zhang, H.W., Huang, X. and Hansen, N. (2008). Evolution of microstructural parameters and flow stresses toward limits in nickel deformed to ultra-high strains. Acta Mater., 56, 5451–5465.

Zhang, Y.B., Mishin, O.V. and Godfrey, A. (2014). Analysis of through-thickness heterogeneities of microstructure and texture in nickel after accumulative roll bonding. J. Mater. Sci., 49, 287–293.

Zhang, Y.B., Mishin, O.V., Kamikawa, N., Godfrey, A., Liu, W. and Liu, Q. (2013). Microstructure and mechanical properties of nickel processed by accumulative roll bonding. Mater. Sci. Eng. A, 576, 160–166.